

Hydrothermal fluid circulation in anisotropic permeable media associated with discrete fractures^①

YANG Jian wen(杨建文)

(School of Earth Sciences, University of Tasmania, Hobart, Tasmania 7001, Australia)

[Abstract] A proper form of the Rayleigh number, containing the geometric mean of the vertical and horizontal permeabilities was obtained. The critical value for the onset of stable convection was found. The results proved analytically and numerically that anisotropy in permeability resists the initiation of hydrothermal convection. The equivalence between homogeneously anisotropic media and multiply fractured media was also investigated. It was confirmed that multiply fractured models are comparable to anisotropic models as long as they have the same averaged horizontal or vertical permeabilities and other physical parameters.

[Key words] hydrothermal fluid circulation; anisotropic permeable media; fractures

[CLC number] P641

[Document code] A

1 INTRODUCTION

Hydrothermal fluid circulation is an important physical phenomenon characteristic on the subsurface of the earth. Among all the controlling parameters, permeability is the most critical variable governing flow within this system. The permeability field is rarely isotropic and homogeneous due to the presence of discrete fractures in the earth structures.

Hydrothermal convection in anisotropic media is a classical problem and several papers have been published by previous researchers. Wooding^[1] investigated the influence of anisotropy and variable viscosity on convection in a heated porous layer. Lowell^[2] derived the condition for the onset of convection in a long, deep, but narrow, vertical fault zone with anisotropic permeability. Kvernold et al^[3] and Tyvand et al^[4] investigated the convection currents in anisotropic porous media, and reported results in steady-state convection. Rosenberg and Spera^[5,6] performed 2-D numerical calculation of finite amplitude and steady convective fluid flow in layered and anisotropic porous media simulating the mid-ocean ridge hydrothermal system, and discussed numerically the relationship among flow, temperature, and anisotropic permeability.

There are two drawbacks of the previous studies. First, the previous studies defined the Rayleigh number R only in terms of the vertical permeability k_z , and did not consider the horizontal permeability k_x . A Rayleigh number should be able to reflect the strength of convection. In other words, the bigger the number was, the stronger the convection should be, and vice versa. However, a definition which depends only on one component of permeability cannot

do this. The second weakness is that they only considered the homogeneously anisotropic porous media and never included discrete fractures, although they recognized that discrete fractures are the major reason for anisotropy in permeability.

This paper contains two parts. First a more useful form of the Rayleigh number, which contains the geometric mean of vertical and horizontal permeabilities, is defined, and an analytical expression for the onset of convection stability in 2-D media is derived. It is confirmed analytically and numerically that anisotropy in permeability resists the initiation of thermal convection. The second part contributes to investigate the equivalence between homogeneously anisotropic media and multiply fractured media. It is confirmed that the latter is comparable to the former if the estimated horizontal and vertical permeabilities as well as other parameters are kept the same.

2 ONSET OF HYDROTHERMAL CONVECTION IN 2-D ANISOTROPIC PERMEABLE MEDIA

The onset of hydrothermal convection in two-dimensional anisotropic permeable media has been studied^[1,3]. The previous studies defined the Rayleigh number only in terms of the vertical permeability k_z . It was expressed as:

$$R = \frac{k_z g \alpha_v \Delta t L}{k_m \nu} \quad (1)$$

Eqn.(1) does not contain the horizontal permeability k_x . But the previous studies did however evaluate a condition for criticality. It is

$$R_c = \pi^2 \left[\left(\frac{k_z}{k_x} \right)^{1/2} + 1 \right]^2 \quad (2)$$

The critical condition on the parameters is $R =$

R_c , then

$$\frac{g\alpha_v\Delta tL}{k_m v} = \pi^2 \left[\frac{1}{k_x} + \frac{1}{k_z} + \frac{2}{\sqrt{k_x k_z}} \right] \quad (3)$$

Based on Eqn.(2), when k_z is less than k_x , the critical Rayleigh number R_c is less than $4\pi^2$ of an isotropic medium, which means that a 2-D anisotropic permeable medium has a less resistance for convection to develop; whereas when k_z is larger than k_x , the critical value is larger than an isotropic medium's value, then 2-D anisotropic permeable medium has a larger resistance for convection to develop. This paradoxical phenomenon originates from ignoring the horizontal permeability in the previous definition of the Rayleigh number.

Consider a 2-D water-saturated anisotropic porous layer with a thickness of L . The layer is heated from the bottom and has a temperature contrast of Δt . When using vertical and horizontal permeabilities as a measure of the bulk permeability of the anisotropic medium, as suggested by Fisher^[7], the Rayleigh number can be written as:

$$R = \frac{\sqrt{k_x k_z} \alpha_v g \Delta t L}{k_m v} \quad (4)$$

Accordingly, the critical Rayleigh number R_c can be derived analytically following the style of Turcotte and Schubert^[8], and the result is

$$R_c = 2\pi^2 + \frac{k_x + k_z}{\sqrt{k_x k_z}} \pi^2 \quad (5)$$

It can be easily proved that the following expression is always true:

$$R_c \geq 4\pi^2 \quad (6)$$

Two points can be immediately drawn from Eqns.(5) and (6). First when 2-D model is isotropic in permeability ($k_x = k_z$), the critical Rayleigh number $R_c = 4\pi^2$, which is exactly the same as previous results. Second, when 2-D model is anisotropic in permeability ($k_x \neq k_z$), the critical Rayleigh number $R_c > 4\pi^2$. In other words, the anisotropic systems have a higher critical Rayleigh number than the isotropic systems.

The critical condition on the parameters can be obtained by inserting Eqn.(4) into Eqn.(5). It is exactly the Eqn.(3).

The previous researches^[9-11] provided the details of the finite element numerical simulation techniques. Here, 2-D models are considered: one is isotropic in permeability, the other is anisotropic with an anisotropic coefficient of 10. The ratio of model

thickness to model width is fixed at 0.5. Other model parameters are given in Table 1. Obviously, these three models have exactly the same geometric shape as well as the averaged permeability ($k_{mean} = 1.8 \times 10^{-10} \text{ m}^2$). It is also assumed these three models have the same initial temperature perturbation and fluid velocity field, as shown in Fig.1.

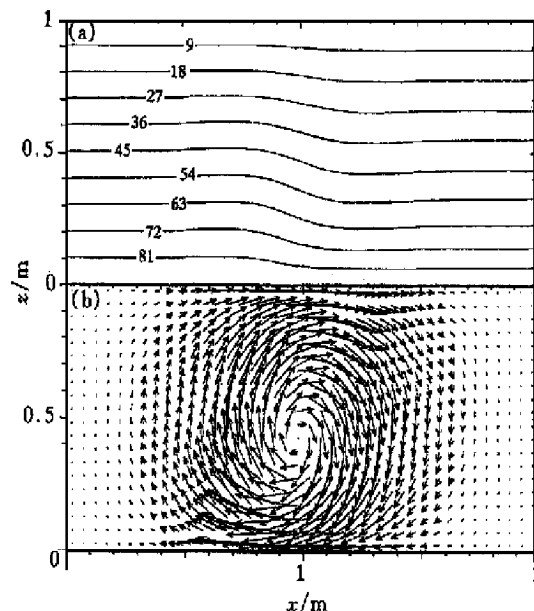


Fig.1 Initial temperature and fluid velocity perturbations for models 1, 2 and 3
(a) — Temperature distribution; (b) — Fluid velocity field (Maximum initial velocity is $3.1 \times 10^{-5} \text{ m/s}$.)

For model 1, since the Rayleigh number R is larger than the critical Rayleigh number R_c , the thermal convection is supposed to happen. The numerical results certainly confirm that the thermal convection occurs. As illustrated in Fig.2(a), the maximum fluid velocity over the simulation domain increases from the initial value v_i , through the higher time levels ($v/v_i = 1.45$ for 0.3 d, $v/v_i = 2.35$ for 0.5 d, and $v/v_i = 3.55$ for 0.7 d), to the steady state ($v/v_i = 4.2$), which implies that the initial temperature or flow perturbation has been amplified, and as time increases, the convection strength becomes stronger, and finally reaches the steady state. Fig.3 shows the temperature distribution and flow field at the steady state. Obviously, there are three convection cells in the domain.

For model 2, since the Rayleigh number R is smaller than the critical Rayleigh number R_c , then the thermal convection will not take place. The nu-

Table 1 Parameters of models 1, 2 and 3

Model	L/m	$\Delta t/^\circ\text{C}$	$\alpha_v/^\circ\text{C}^{-1}$	$v/(m^2 \cdot s^{-1})$	$k_m/(m^2 \cdot s^{-1})$	k_x/m^2	k_z/m^2	R_c	R
Model 1	1.0	90.0	8×10^{-4}	1.787×10^{-6}	7.187×10^{-7}	1.8×10^{-10}	1.8×10^{-10}	40.0	100.0
Model 2	1.0	90.0	8×10^{-4}	1.787×10^{-6}	7.187×10^{-7}	1.8×10^{-11}	1.8×10^{-9}	119.0	100.0
Model 3	1.0	90.0	8×10^{-4}	1.787×10^{-6}	7.187×10^{-7}	1.8×10^{-9}	1.8×10^{-11}	119.0	100.0

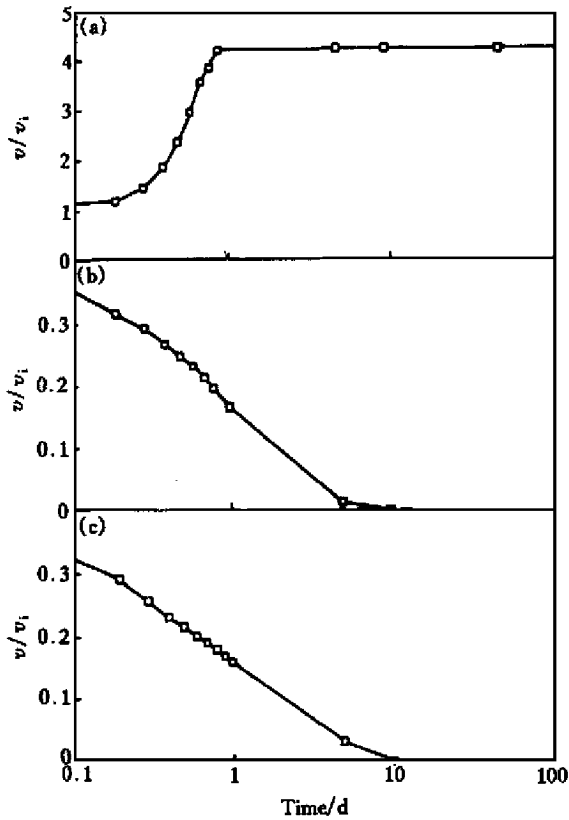


Fig.2 Curves of fluid velocity vs time
(a) — Model 1 ; (2 — Model 2 ; (3) — Model 3

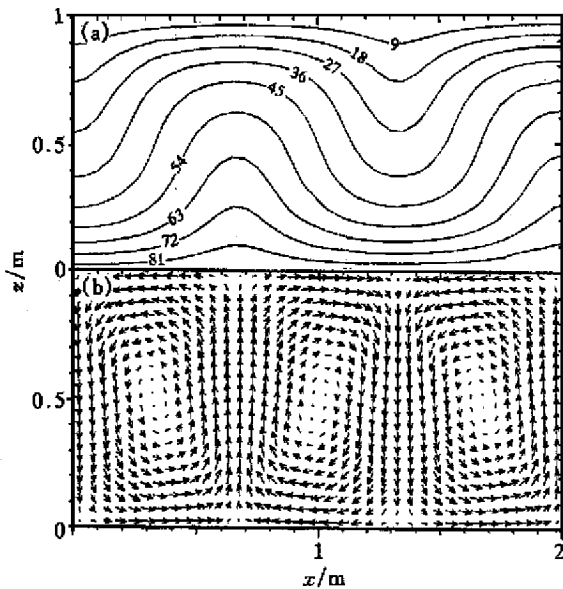


Fig.3 Numerical simulation results at steady state for model 1
(a) — Temperature distribution ; (b) — Fluid velocity field
(Maximum fluid velocity is now up to 1.3×10^{-4} m/s.)

numerical results indeed prove that the model inhibits the initiation of thermal convection, as shown in Fig. 2(b), the maximum fluid velocity decreases from the initial value v_i , through the higher time levels ($v/v_i = 0.24$ for 0.5 d, $v/v_i = 0.16$ for 1.0 d, $v/v_i = 9.7$

$\times 10^{-4}$ for 10.0 d, and $v/v_i = 2.12 \times 10^{-5}$ for 50.0 d), to the steady state ($v/v_i = 0$), which means that the initial temperature or fluid motion perturbation has been inhibited. As time increases, the strength of thermal convection becomes weaker, and finally reaches the steady state without any convection. Fig.4 shows the temperature distribution at the steady state. Clearly, the initial temperature perturbation shown in Fig.1 has been flattened, and the temperature contours now are a set of perfectly horizontal lines, which means that the conductive mechanism of heat transport is dominant.

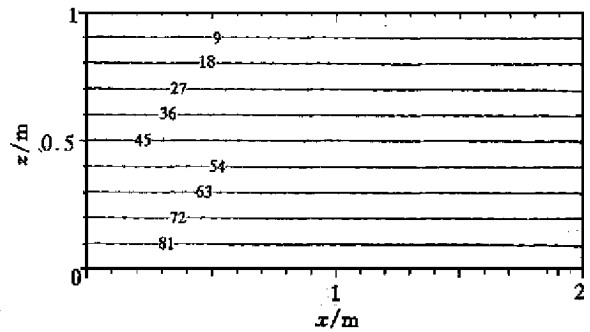


Fig.4 Temperature distributions at steady state for models 2 and 3
(Convective effect is now negligible)

Model 3 is similar to model 2 with the anisotropy reversed. The thermal convection will not happen due to $R = 100$, which is smaller than $R_c = 119$. The numerical results again confirm the prediction. The maximum fluid velocity also decreases down to zero from the initial value to the steady state limit, as illustrated in Fig.2(c). The temperature of the steady state are exactly the same as what is shown in Fig.4.

3 EQUIVALENCE BETWEEN HOMOGENOUSLY ANISOTROPIC MEDIA AND MULTIPLY FRACTURED MEDIA

Consider a 2-D water-saturated system with a dimension of 10 m \times 20 m. The solution domain is discretized by a 2-D equal-spaced grid. There are 40 and 20 elements in x and z directions, respectively. All four boundaries are assumed impermeable. The temperatures of the upper and lower boundaries are fixed at 0 °C and 10 °C, respectively. The side boundaries are assumed adiabatic. Thermal conductivity and porosity are assigned to 3.6 J/s and 10%, respectively.

Open fracture permeability is mainly dependent on its aperture $2b$, and it is usually much larger than the permeability of host medium. Thus, the multiply fractured porous medium, as a whole, is made up of alternative layers with different permeabilities. For these types of materials, the effective average hori-

horizontal and vertical permeabilities can be estimated^{d41}. When the alternative layers are in vertical direction, they are

$$k_x = 1 / \left(\sum_{i=1}^N \frac{d_i}{dk_i} \right) \tag{7}$$

$$k_z = \sum_{i=1}^N \frac{d_i}{d} k_i \tag{8}$$

where d_i and k_i are the thickness and permeability of the layer i ($i = 1, 2, \dots, N$), with N being the total number of layers making up the total thickness d .

For an orthogonally multiply fractured model, assume that the host medium is impermeable and there are 390.85 mm wide vertical fractures rising from the bottom to the top, and 190.86 mm wide horizontal fractures spanning from wall to the right wall. These two fractures are spaced uniformly. Although the host medium itself is impermeable, the interconnected fractures provide the paths for hydrothermal fluid circulation. It can be estimated that both k_x and k_z are equal to 10^{-10} m^2 . Thus, the system as a whole is isotropic in permeability. Now assume there are no discrete fractures, but the host medium is permeable and has a permeability of 10^{-10} m^2 , keeping other parameters and conditions intact. The Rayleigh number for both systems are 50, larger than the critical value. Hydrothermal convection can be initiated and maintained. The numerical simulations at steady state are shown in Fig. 5. Figs. 5(a) and (c) are temperature contours and the homoge-

neously isotropic model, Figs. 5(b) and (d) are fluid velocity fields, where, (a) and (b) correspond to the orthogonally multiply fractured model, (c) and (d) correspond to the homogeneously isotropic model. The averaged relative error between Figs. 5(a) and (c) equals to 1.55%.

For vertically multiply fractured model, the host medium is assigned a permeability of 10^{-10} m^2 and there are 39 uniformly spaced vertical fractures rising from the bottom to the top. Other conditions are kept the same. When the fracture aperture $2b$ is 1.0, 1.5 and 2.0 mm, the estimated average vertical permeabilities are accordingly 2.63×10^{-10} , 6.48×10^{-10} and $14.00 \times 10^{-10} \text{ m}^2$, but the estimated average horizontal permeabilities are all 10^{-10} m^2 . The numerical simulation results for the model at steady state are shown in Fig. 6 correspond to $2b = 1.5 \text{ mm}$. For a uniformly anisotropic porous model with a fixed horizontal permeability of 10^{-10} m^2 , the vertical permeability is 2.63×10^{-10} , 6.48×10^{-10} and $14.00 \times 10^{-10} \text{ m}^2$. The steady state numerical simulation result with vertical permeability of $6.48 \times 10^{-10} \text{ m}^2$ are shown in Fig. 7. It can be seen that when fracture aperture $2b$ increases, the effective vertical permeabilities become larger, the temperature contours seem to have been compressed more in the horizontal direction, and the convection cells in host medium become thinner and narrower. This is not surprising because the existence of the vertical fractures leads to

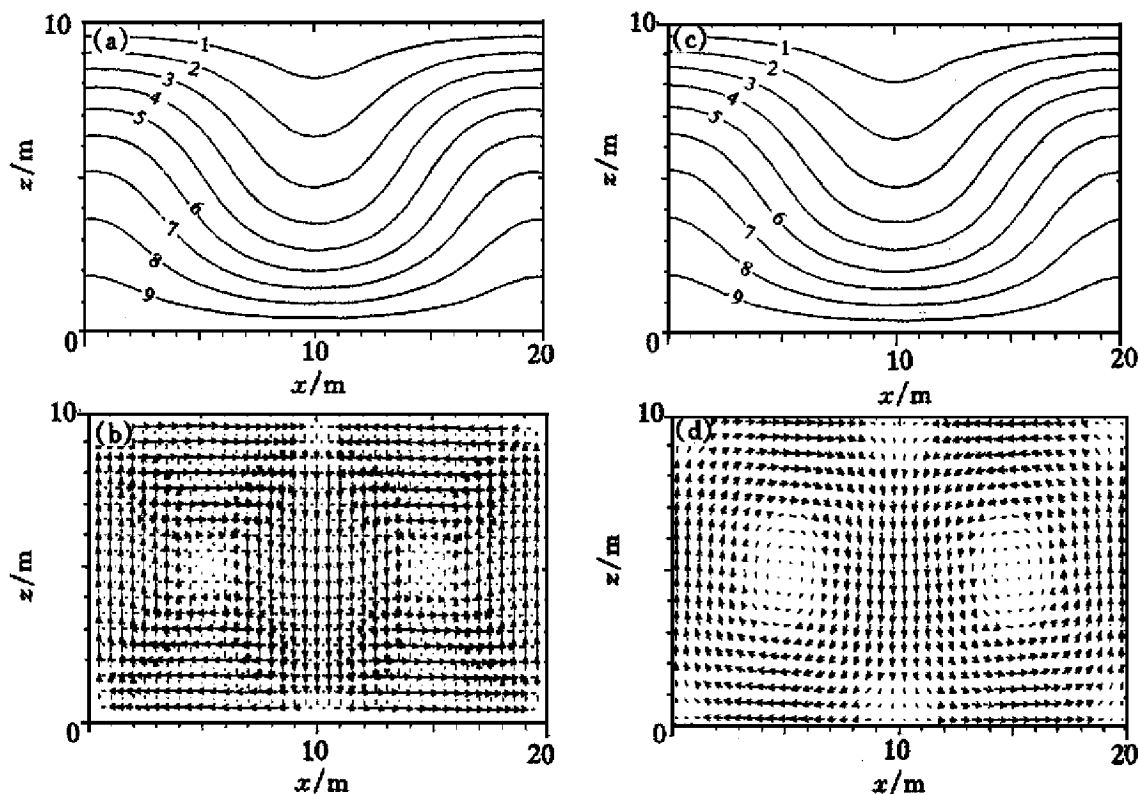


Fig. 5 Numerical simulation results at steady state
 (a), (c) — Temperature contours; (b), (d) — Fluid velocity fields

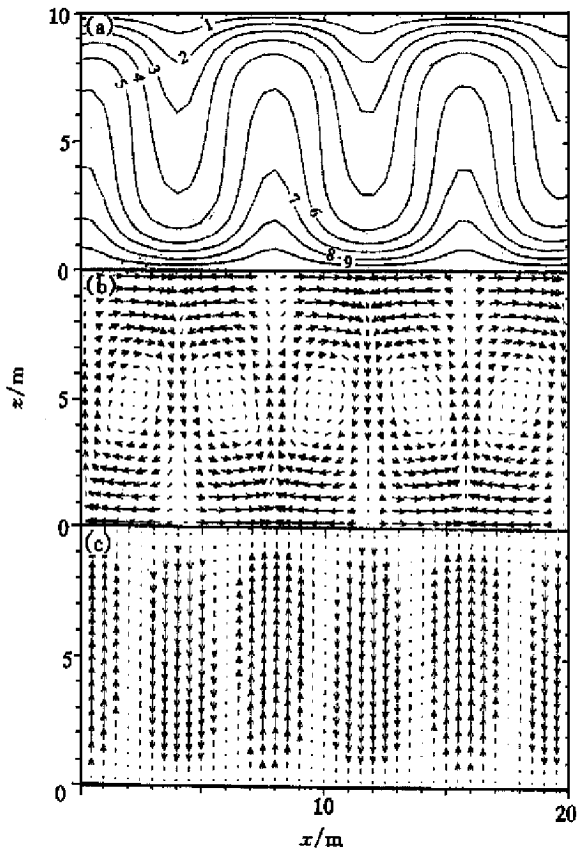


Fig. 6 Numerical simulation results for vertically multiply fractured model at steady state
 (a) — Temperature contours;
 (b) — Fluid velocity field in host medium;
 (c) — Fluid velocity field in discrete fractures

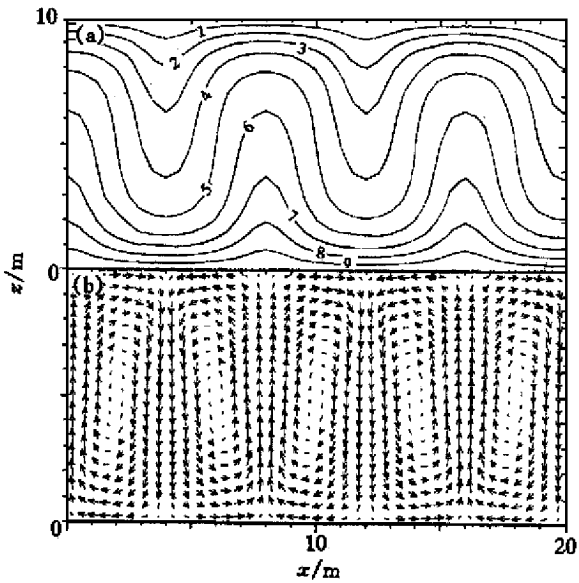


Fig. 7 Numerical simulation results for homogeneously anisotropic medium
 (a) — Temperature contours; (b) — Fluid velocity field

less hydraulic resistance in vertical direction, so fluid flows more easily in the vertical direction than the

horizontal direction. It also can be concluded that the vertical discrete fractures mainly contribute to the vertical transport of fluid, whereas the host porous medium is most responsible for the horizontal transport of fluid between the adjacent fractures. Also, the results of the vertically multiply fractured models are comparable to those of the homogeneously anisotropic models.

For horizontally multiply fractured model, the host medium is assigned a permeability of 10^{-10} m^2 and there are 19 uniformly spaced horizontal fractures across the model from the left to the right. These fractures have an aperture of 1.5 mm. Other conditions are kept the same. The estimated average horizontal and vertical permeabilities are 6.43×10^{-10} and 10^{-10} m^2 , respectively. The numerical simulation results are shown in Fig. 8. For uniformly anisotropic porous model, the fixed horizontal and vertical permeabilities are $6.34 \times 10^{-10} \text{ m}^2$ and 10^{-10} m^2 , respectively. The simulation results are shown in Fig. 9. Now the temperature contours seem to have been stretched along the horizontal direction. Only one convection cell has been formed in the host porous medium. The shape of the convection cell now becomes long and flat with an aspect ratio of about 2.

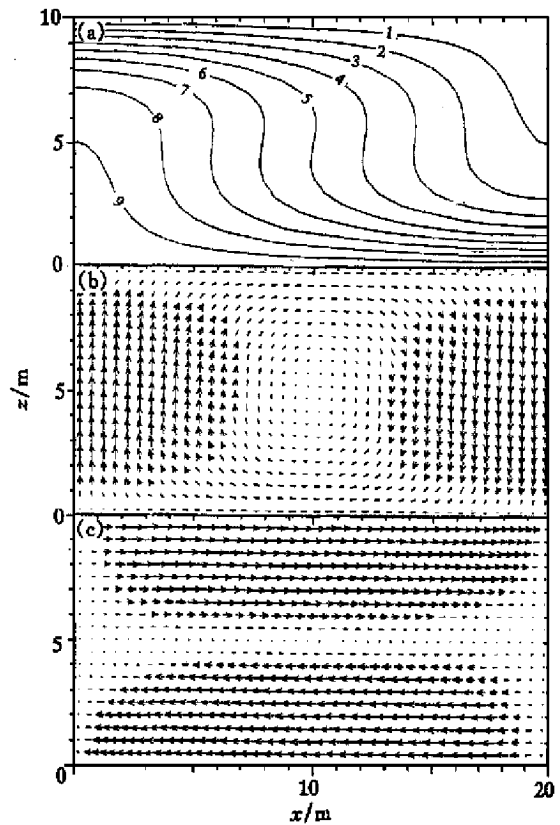


Fig. 8 Numerical simulation results for horizontally multiply fractured model at steady state
 (a) — Temperature contours;
 (b) — Fluid velocity field in host medium;
 (c) — Fluid velocity field in discrete fractures

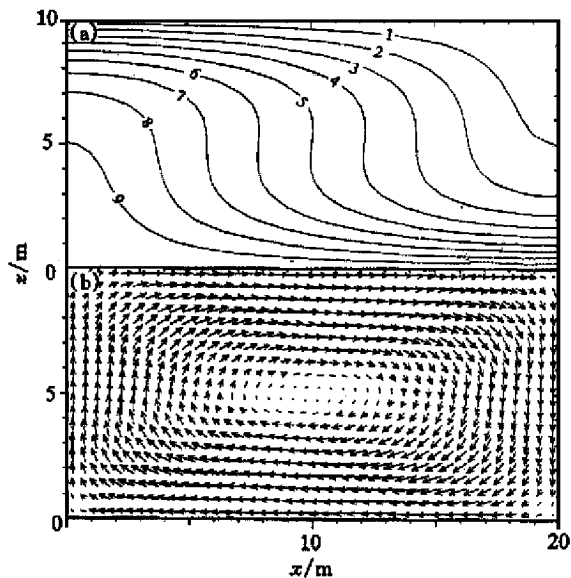


Fig. 9 Numerical simulation results for homogeneously anisotropic medium
(a) — Temperature contours ; (b) — Fluid velocity field

This is also reasonable because the horizontal fractures lead to less hydraulic resistance for fluid motion. The results in Fig. 8 indicate that the horizontal fractures mainly contribute to the horizontal fluid transport, whereas the host porous medium provide a surplus for the vertical fluid transport between the adjacent fractures. Again the results of the horizontally multiply fractured model are comparable to those of the homogeneously anisotropic model. The average relative error between Figs. 8(a) and 9(a) is 2.36%.

4 CONCLUSIONS

Hydrothermal circulation in 2-D anisotropic permeable media associated with discrete fractures has been investigated both analytically and numerically. A more useful form of the Rayleigh number has been defined, containing the geometric mean of vertical and horizontal permeabilities. The critical value of this form Rayleigh number for the onset of hydrothermal convection has been provided, and it is higher than that for isotropic media. The larger the anisotropic coefficient is, the higher the critical Rayleigh number is, which indicates that the anisotropy in permeability resists the initiation of thermal convection. Numerical experiments have confirmed this conclusion.

The numerical simulation results have indicated that even if the host medium is impermeable, the presence of the interconnected discrete fractures can promote hydrothermal convection. The multiply frac-

tured porous media are comparable with the homogeneously anisotropic media in the numerical solutions if the effective average horizontal and vertical permeabilities are kept the same. Temperature contours are compressed along the horizontal direction and convection cells become thin and narrow when there exists a set of vertical fractures, hence the vertical permeability is higher than the horizontal one; on the other hand, temperature contours are stretched along the horizontal direction, and convection cells become flat and long when there exists a set of horizontal fractures, hence the horizontal permeability is higher than the vertical one.

[REFERENCES]

- [1] Woolding R A. Influence of anisotropy and variable viscosity upon convection in a heated saturated porous layer [R]. Department of Scientific and Industrial Research, Technical Report No. 55 [R], Wellington, New Zealand, 1976.
- [2] Lowell R P. The onset of convection in a fault zone: effect of anisotropic permeability [J]. Geothermal Resources Council, Transactions, 1979, 3: 337 - 370.
- [3] Kvernovold O and Tyvand P A. Nonlinear thermal convection in anisotropic porous media [J]. Fluid Mech, 1979, 90: 609 - 624.
- [4] McKibbin R and Tyvand P A. Thermal convection in a porous medium with horizontal cracks [J]. Int J Heat Mass Transfer, 1984, 27: 1007 - 1023.
- [5] Rosenberg N D and Spera F J. Role of anisotropic and/or layered permeability in hydrothermal systems [J]. Geophys Res Lett, 1990, 17: 235 - 238.
- [6] Rosenberg N D, Spera F J and Haymon R M. The relationship between flow and permeability field in seafloor hydrothermal systems [J]. Earth Planet Sci Lett, 1993, 116: 135 - 153.
- [7] Fisher A T, Becker K and Narasimhan T N. Off-axis hydrothermal circulation: parametric tests of a refined model of processes at Deep Sea Drilling Project/ Ocean Drilling Program site 504B [J]. J Geophys Res, 1994, 99: 3097 - 3121.
- [8] YANG Jiar-wen, Latychev K and Edwards R N. Numerical computation of hydrothermal fluid circulation in fractured Earth structures [J]. Geophys J Int, 1998, 135: 627 - 649.
- [9] YANG Jiar-wen. Numerical simulation of hydrothermal convection within discretely fractured porous media [D]. Canada: University of Toronto, 1996.
- [10] YANG Jiar-wen, Edwards R N, Molson J W, et al. Three-dimensional numerical simulation of the hydrothermal system within the TAG-like sulfide mound [J]. Geophys Res Lett, 1996, 23 (23) A: 3475 - 3478.
- [11] YANG Jiar-wen, Edwards R N, Molson J W, et al. Fracture-induced hydrothermal convection in the oceanic crust and the interpretation of heat-flow data [J]. Geophys Res Lett, 1996, 23(9) B: 929 - 932.

(Edited by LONG Huai-zhong)